EurJIC
European Journal of Inorganic Chemistry

A Journal of
ChemPubSoc Europe

Accepted Article

Title: Effects of multi-carborane substitution on the photophysical and electron accepting properties of o-carboranylbenzene compounds

Authors: Dong Kyun You, Ji Hye Lee, Byung Hoon Choi, Hyonseok Hwang, Min Hyung Lee, Kang Mun Lee, and Myung Hwan Park

To be cited as: *Eur. J. Inorg. Chem.* 10.1002/ejic.201700192

Link to VoR: http://dx.doi.org/10.1002/ejic.201700192

WILEY-VCH

Effects of multi-carborane substitution on the photophysical and electron accepting properties of *o*-carboranylbenzene compounds

Dong Kyun You,[a]† Ji Hye Lee,[a]† Byung Hoon Choi,[a] Hyonseok Hwang,[a] Min Hyung Lee,*[b] Kang Mun Lee,*[a] and Myung Hwan Park*[c]

Abstract: Multiple *o*-carborane substituted compounds, mono-, 1,3-bis-, and 1,3,5-tris-(2-(4-butylphenyl)-*o*-carboran-1-yl)benzene (**1**–**3**), were prepared and characterized by multinuclear NMR spectroscopy and elemental analysis. The solid-state structures of **2** and **3** were also confirmed by single crystal X-ray diffraction. While the mono-carborane compound **1** was non-emissive in solution state at 298 K, the photoluminescence (PL) spectra of **2** and **3** exhibited weak to moderate emission (λ_{em} = 352 nm for **2** and 363 nm for **3** in THF). Compounds **2** and **3** showed intriguing dual emission bands (λ_{em} = 361 and 537 nm for **2** and λ_{em} = 387 and 520 nm for **3**) at 77 K and in film, of which the low-energy band was dominant in the solid state. TD-DFT calculations on the S_1 optimized structures suggested that the low-energy fluorescence of **2** and **3** was attributed to the π(4-butylphenyl) → π*(phenylene-*o*-carborane) intramolecular charge transfer (ICT) transition. The low-energy electronic transition of **2** and **3** was apparently associated with an aggregation-induced emission (AIE), and enhanced emission intensity (λ_{em} = *ca.* 570 nm for **2** and λ_{em} = *ca.* 550 nm for **3**) was observed upon increasing the water fraction (f_w) in THF/water mixtures. Furthermore, the PL experiments of poly(3-hexylthiophene-2,5-diyl) (P3HT) polymer films doped with **3** revealed the excellent electron-accepting properties of **3**.

Introduction

Icosahedral carboranes ($C_2B_{10}H_{12}$) are well-known boron-cluster compounds that can be often characterized as three-dimensional (3D) analogues to aromatic derivatives.[1] Because of these unique properties, carboranyl compounds have been utilized as functional materials for a wide range of applications.[2] In particular, *o*-carborane (*closo*-1,2-$C_2B_{10}H_{12}$)-appended compounds have recently attracted great interest for optoelectronic applications due to their unique luminescent properties and high thermal/chemical stabilities.[3-5] These intriguing properties are attributed to the intrinsic nature of the *o*-carborane units, such as strong electron-withdrawing effects through the C atom on the cage and highly polarizable σ-aromatic characters,[6] leading to the expansion of their utilization as promising luminescent materials.[7] To date, in order to induce fascinating photophysical properties, structural modifications have been made through the incorporation of *o*-carborane groups into transition-metal complexes[8-12] or organic luminophores.[13] In particular, *o*-carborane-incorporated organic luminophores often exhibit unusual multiple emission behaviour derived from discrete intramolecular charge transfer (ICT) and locally excited (LE) states.[13-25] These features have been mainly observed in the donor-acceptor dyad systems in which the *o*-carborane group acts as an acceptor. For example, Kang and co-workers have reported donor-acceptor dyads (**I** in Figure 1) having carbazole units as a donor, demonstrating unique charge-separated excited states between the individual moieties.[14,15] Fox *et al.* have also reported *C*-diazaboryl-*o*-carborane dyads (**II**) exhibiting dual emissions from high- energy LE and low-energy CT states depending on the substituents and molecular geometry.[16,17] Furthermore, *o*-carborane derivatives

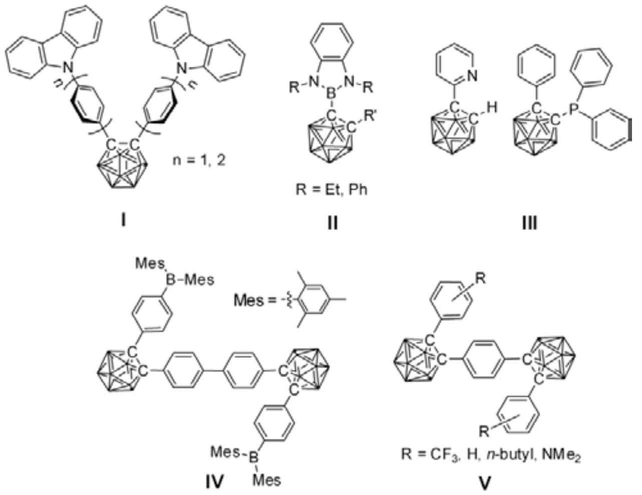

Figure 1. *o*-Carborane derivatives exhibiting multiple emission behaviour.

---

[a] Dr. J. H. Lee, D. K. You, B. H. Choi, Prof. Dr. H. Hwang, Prof. Dr. K. M. Lee
Department of Chemistry
Institute for Molecular Science and Fusion Technology
Kangwon National University, Chuncheon, Gangwon 24341
Republic of Korea
E-mail: kangmunlee@kangwon.ac.kr
[b] Prof. Dr. M. H. Lee
Department of Chemistry and EHSRC
University of Ulsan, Ulsan 44610
Republic of Korea
E-mail: lmh74@ulsan.ac.kr
[c] Prof. Dr. M. H. Park
Department of Chemistry Education
Chungbuk National University, Cheongju, Chungbuk 28644
Republic of Korea
E-mail: mhpark98@chungbuk.ac.kr
† These authors contributed equally to this work

Supporting information for this article is given via a link at the end of the document.

(**III**) with 2-pyridyl or diphenylphosphino groups displayed multi-emission features via different excited states.[25] Recently, we have reported that a biphenylene-bridged dimeric *o*-carboranyl triarylborane compound (**IV**) can show dual emissions resulting from a triarylborane-based LE and an ICT-based aggregation-induced emission (AIE) in a rigid state.[13a] We also found that "through-space" ICT between the appended aryl group and the central phenylene ring can lead to emission color tuning of *para*-di-*o*-carboranylbenzene compounds (**V**) depending on the type of substituent on the appended aryl group.[18]

Although these emission behaviors in π-substituted *o*-carborane derivatives have been extensively examined, detailed investigation on the photophysical properties caused by the alteration of the number of *o*-carborane units has not been reported. The introduction of multi-carborane units into a molecule could not only give rise to systematic variation of optical properties, but also enhance electron-accepting ability. The latter property could also be promising for optoelectronic applications such as organic field-effect transistors (OFETs) and organic photovoltaics (OPVs).[26] In an effort to investigate the electronic effects of *o*-carborane and the photophysical properties of the resulting aryl-*o*-carborane compounds, we herein report mono-, bis-, and tris-*o*-carboranylbenzene (**1**–**3**) compounds and their luminescent/electron-accepting properties along with computational details.

Results and Discussion

Synthesis and characterization. The bis-acetylene (**2a**) and tris-acetylene (**3a**) precursors were readily obtained from the palladium-catalyzed Sonogashira coupling reactions of 1,3-dibromobenzene and 1,3,5-tribromobenzene with 4-butylphenylacetylene, respectively (Scheme 1). The final bis- and tris-carborane compounds (**2** and **3**) were prepared from the well-known boron cage forming reaction of decaborane ($B_{10}H_{14}$) with the acetylene precursors (**2a** and **3a**) in the presence of excess Et_2S (yield = 33% for **2** and 46% for **3**). Note that the *n*-Bu group was introduced to the 2-phenyl substituent of *o*-carborane to endow high solubility in common organic solvents. In addition, mono-carborane compound **1** was also similarly prepared to compare the effects of multi-*o*-carborane substitution on the luminescent properties.

The formation of **1**−**3** was characterized by multinuclear NMR spectroscopy (Figure S15−S23 in the Supporting Information), high resolution mass spectroscopy, and elemental analysis. ^{1}H and ^{13}C NMR spectra of **1**−**3** exhibited the expected resonances corresponding to the 2-aryl-*o*-carboranyl (aryl = 4-*n*-BuPh) and central phenylene moieties. The ^{11}B NMR signals of **1**–**3** detected in the region of δ −1 to −11 ppm confirmed the presence of *o*-carboranyl boron atoms. Moreover, the ^{11}B NMR spectra of **1**–**3** distinctly exhibited two coupled peak sets in an integral ratio of 3:7, although less resolved splitting patterns for **2** and **3** even at 60 °C (Figures S17, S20, and S23 in the Supporting Information). The B–H coupling constants ($^{1}J_{B-H}$) of ca. 126–166 Hz are also similar to the range observed for carborane compounds.[27] Single crystals of **2** and **3** suitable for X-ray diffraction analyses were obtained from a CH_2Cl_2/*n*-hexane solution at −20 °C (Figure 2). While bis-carborane compound **2** has *syn* conformation, tris-carborane compound **3** shows C_1 symmetry and *anti*-stereochemistry, in which one 2-Ar group is oriented to the opposite side of the others, probably due to steric congestion between the 2-Ar groups. The *anti*-conformation of **3** is in contrast to the previously reported crystal structure of 1,3,5-tris(2-Ph-*o*-carboran-1-yl)benzene compound without *n*-Bu group in the phenyl ring, which possessed C_3 symmetry and *syn* stereochemistry of three phenyl groups.[28] The substantial torsion angles of C_{cage}–C_{cage}–C_{Ph}–C_{Ph} in **2** (ψ = 51.3°) and **3** (ψ = 66.7°) can be mainly ascribed to the steric hindrance between the 2-Ar and central phenylene rings.

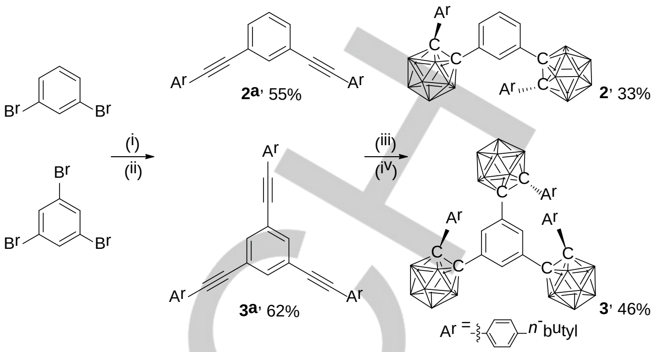

Scheme 1. Synthetic routes for **2** and **3**. Reagents and conditions: (i) $Pd(PPh_3)_2Cl_2$, CuI, triethylamine, 4-butylphenylacetylene. (ii) toluene, 110 °C, 24 h. (iii) $B_{10}H_{14}$, Et_2S. (iv) toluene, 110 °C, 72 h.

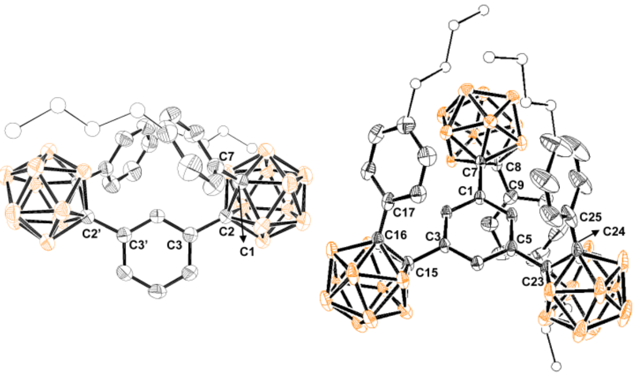

Figure 2. X-ray crystal structures of **2** (left) and **3** (right) (40% thermal ellipsoids). The H atoms are omitted for clarity.

Thermal and electrochemical stabilities. The thermal stabilities of the bis- and tris-carborane compounds (**2** and **3**) were examined by thermogravimetric analysis (TGA) (Figure 3a and Table 1). Compounds **2** and **3** exhibited T_{d5} values of 361 and 376 °C, respectively, indicating high thermal stability. Inherited from high thermal stability of *o*-carborane cage, the T_{d5}

Table 1. Photophysical and electrochemical data of **1**–**3**

	λ_{abs}[a] /nm (log ε)	$\lambda_{em.max}$ [nm]								Φ_{em}		E_{red}[h] /V	LUMO[i] /eV	T_{d5}[j] /°C
		Cyhex[b]	THF[b]		DMSO[b]	film[c,d]	Solid[d]	f_w = 90 %[d,e]						
		298 K	298 K	77 K	298 K					THF[b,f]	Solid[g]			
1	233 (3.94), 273 (3.78)	_[k]	_[k]		_[k]	_[k]				_[k]		−1.99	−2.81	
2	213 (4.67)	327	352	361, 537	363	380, 538	539	573		0.040	0.097	−1.49	−3.31	361
3	229 (4.81)	337	363	387, 520	376	382, 520	521	546		0.147	0.102	−1.27	−3.53	376

[a] $c = 5.0 \times 10^{-5}$ M in THF. [b] $c = 5.0 \times 10^{-5}$ M, determined at 298 K (Excitation, λ_{ex} = 290 nm for **1**, 296 nm for **2**, and 309 nm for **3**). [c] PMMA film doped with 20 wt% of compound. [d] λ_{ex} = 340 nm. [e] $c = 5.0 \times 10^{-4}$ M. [f] Quinine sulfate (Φ = 0.55) used as a standard. [g] Absolute photoluminescence quantum yield. [h] The reduction onset potential in DMSO ($c = 5.0 \times 10^{-4}$ M, scan rate = 100 mVs^{-1}) with reference to the ferrocene/ferrocenium (Fc/Fc$^+$) redox couple. [i] Calculated from the E_{red}. [j] Determined by TGA at 5% weight loss. [k] Not observed.

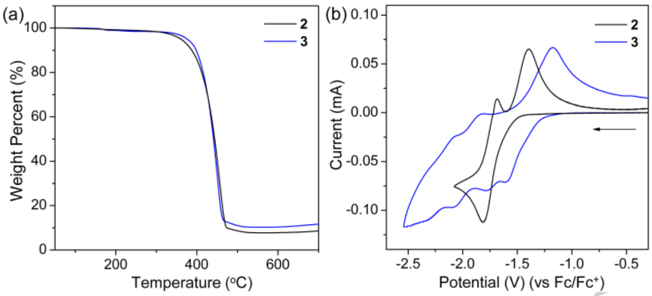

Figure 3. (a) TGA curves and (b) cyclic voltammograms (0.5 mM in DMSO, scan rate = 100 mV s^{-1}) of **2** and **3**.

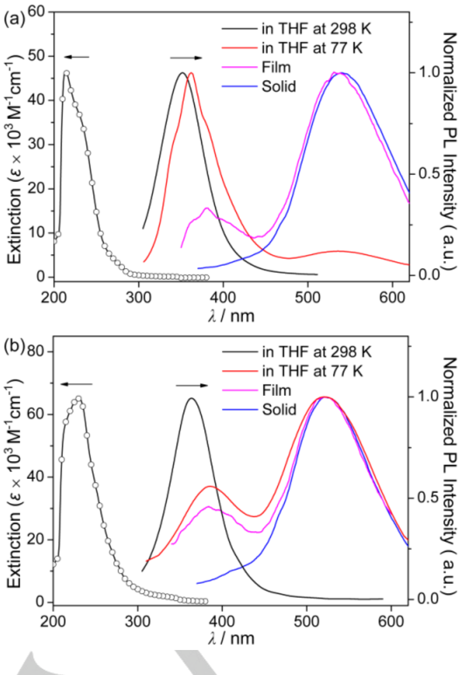

Figure 4. UV/Vis absorption in THF and PL spectra for (a) **2** and (b) **3**.

value of tris-substituted **3** was also higher than that of bis-substituted **2**.

The electrochemical properties of **2** and **3** were investigated by cyclic voltammetry (CV) measurements (Figure 3b and Table 1). Both **2** and **3** showed carborane-centred, quasi-reversible reduction behaviour (E_{red} = −1.49 and −1.27 V, respectively), which is similar to the typical characteristic of 1,2-di-aryl-*o*-caborane compounds.[29,30] To examine the effect of increment in the number of *o*-carborane groups, the reduction potential (E_{red} = −2.01 V) of a mono-*o*-carboranylbenzene compound (**1**) was further measured (Figure S1a in the Supporting Information). According to the reduction potentials of **1**–**3**, which show gradual anodic shifts with the number of *o*-carborane groups, the LUMO energy levels for **1**–**3** were estimated to be −2.79, −3.31, and −3.53 eV, respectively. These results clearly indicate the increased stabilization of LUMO level with the increasing number of 2-Ar-*o*-carborane groups. This could be attributed to not only the enhanced inductive electron-withdrawing effects by the *o*-carborane groups, but also the conjugation effects of *o*-carboranes.[4b,8,10] Furthermore, multiple CV cycles revealed the high electrochemical stability of **1**–**3** (Figure S1 in the Supporting Information).

Optical properties. The optical properties of **1**–**3** were examined by UV/Vis absorption and photoluminescence (PL) measurements. The absorption spectra of **2** (λ_{abs} = 213 nm) and **3** (λ_{abs} = 229 nm) in THF exhibited intense absorption in the range of 210–250 nm mainly assignable to ππ* transition in the central phenylene and the appended 2-Ar rings (Figure 4 and Table 1). In addition, **2** and **3** showed weak low-energy absorption from *ca.* 275 nm to *ca.* 350 nm with the more red-shifted feature in **3**. These low- energy tails could be tentatively assigned to π(2-Ar) → π*(central phenylene) charge transfer (CT) transitions in nature (see TD-DFT results below). Similar weak low-energy absorption (λ_{abs} = 250–325 nm, ε < 6000 M^{-1}) was also observed for **1** (Figure S2 in the Supporting Information). These absorption features are similar to those of the *para*-substituted di-*o*-carborane compounds.[18]

Next, the PL spectra of **1**–**3** were measured in solution and solid state (Figure 4 and Table 1). In contrast to the non-

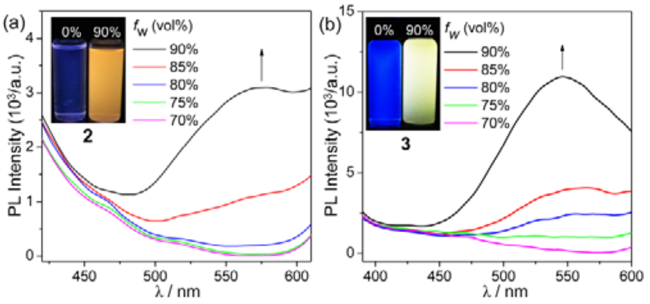

Figure 5. PL spectra of (a) **2** and (b) **3** in THF–water mixtures (5.0×10^{-4} M, $\lambda_{ex} = 340$ nm). Inset shows the emission colour of **2** and **3** in 0% or 90% water mixtures under a hand-held UV lamp ($\lambda_{ex} = 365$ nm).

emissive nature of **1** in solution state, the emission spectra of **2** and **3** in THF at 298 K exhibited weak to moderate emission bands (λ_{em} = 352 nm for **2** and 363 nm for **3**). This feature is different from that found for the *para*-substituted di-*o*-carborane compounds,[18] as well as other *o*-carborane derivatives,[15,29a,31-36] which are almost non-emissive in solution. For the *para*-substituted di-*o*-carboranes, it was suggested that the substantial conjugation between two carborane cages and a central phenylene ring, which is coupled with the C–C bond variation of *o*-carborane, was responsible for the emission quenching in solution.[18] Thus, the distinct emission bands observed for **2** and **3** in solution could be attributed to the weak conjugation between the central phenylene ring and the *meta*-substituted carborane cages. As similarly observed in the absorption spectra, the position of the emission band for tris-carborane substituted **3** was red-shifted as compared to that for bis-substituted **2**. The narrower band gap for **3** than for **2** can be related to the greater LUMO stabilization in the former by the three carborane moieties, as shown in the reduction potential measurements. Furthermore, the quantum efficiency of **3** (Φ_{em} = 0.147) was much higher than that of **2** (Φ_{em} = 0.040) in THF. Note that the mono-substituted **1** was non-emissive in THF. This finding indicates that the increase in the number of *o*-carborane units could enhance the quantum efficiency. This might be partly ascribed to the increased steric congestion between the 2-Ar-*o*-carborane moieties, restricting the free rotation of the carborane moieties.[16,17] Additional PL experiments of **2** and **3** were performed in solvents of different polarities (Table 1 and Figure S3 in the Supporting Information). The emission spectra of **2** and **3** clearly showed bathochromic shifts with increasing solvent polarity, indicating polarized excited states in **2** and **3**. Along with the broad featureless emission bands, these results indicate that the emissive excited states of **2** and **3** in solution bear a CT character.

Most interestingly, **2** (*ca.* 370 nm and 538 nm) and **3** (*ca.* 380 nm and 510 nm) exhibited dual emission bands (Figure 4 and Table 1) in a rigid state, such as at 77 K and in film,

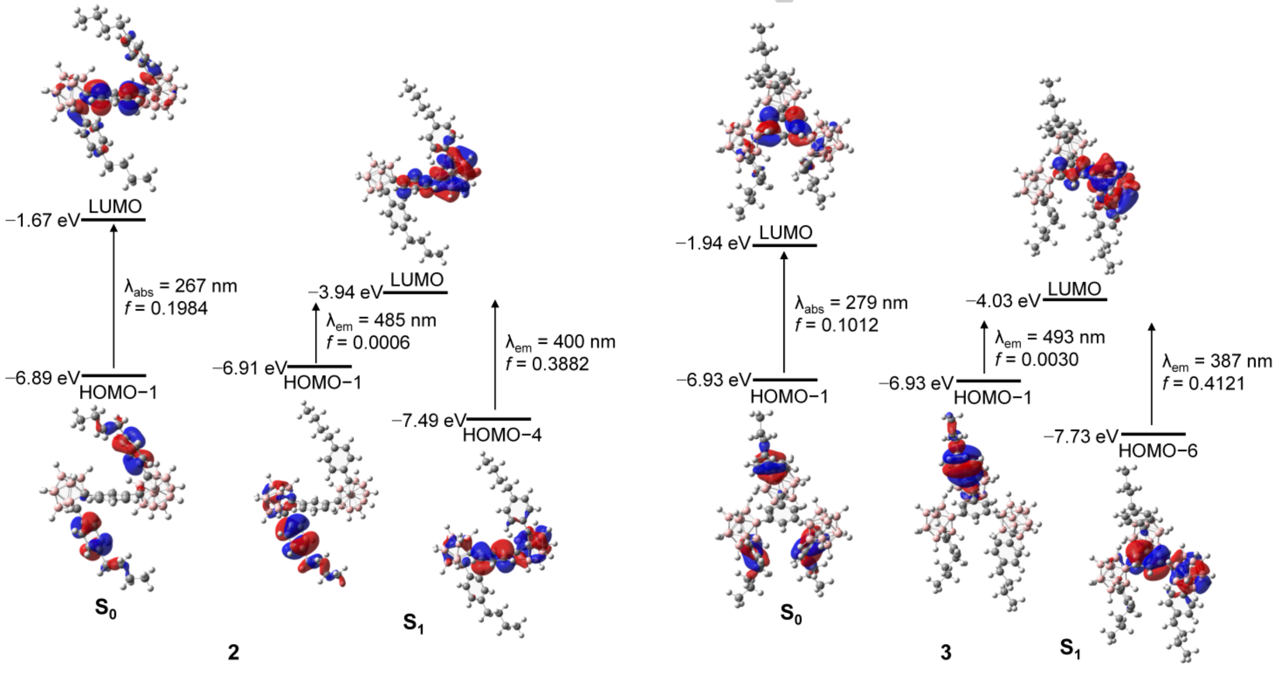

Figure 6. Frontier molecular orbitals for **2** and **3** at their ground state (S_0) and first excited singlet state (S_1) with their relative energies from DFT calculation. The transition energy (in nm) was calculated using the TD-B3LYP method with 6-31G(d) basis sets.

although the intensities of the high-energy and low-energy bands are differently observed for **2** and **3** at 77 K. In addition, a broad low-energy emission band was dominantly observed in the solid state (λ_{em} = 539 nm for **2** and λ_{em} = 521 nm for **3**). The high-energy emission bands for **2** and **3** in the rigid state were similar to those observed in solution, indicating the same origin of emission. Thus, the low-energy emission observed for **2** and **3** in the rigid state and solid state could be involved with aggregation-induced emission (AIE), as in the case of previously reported *o*-carborane-appended luminophores.[7a,13a,16–18,33] To clarify the AIE phenomenon in **2** and **3**, PL experiments were performed in THF–water mixed solvents (Figure 5). The emission intensity of **2** and **3** was remarkably enhanced upon increasing the water fraction (f_w) in THF–H_2O mixtures. In particular, when f_w is as high as 90%, the intensity of the broad low-energy emission (*ca.* 570 nm for **2** and 550 nm for **3**) was maximized. Consequently, while the compound **2** and **3** showed blue emission in THF, aggregates of **2** and **3** in a THF–H_2O (f_w = 90%) mixture exhibited orange and yellow fluorescence, respectively, similar to the low-energy emission bands in the solid state above. Furthermore, the quantum efficiency of **2** (Φ_{em} = 0.097) in solid was comparable to that of **3** (Φ_{em} = 0.102).

Theoretical calculation. To elucidate the absorption and emission features of **2** and **3**, TD-DFT calculations on the ground state (S_0) and first excited state (S_1) optimized structures were performed with the B3LYP functional and 6-31G(d) basis sets (Figure 6 and Table 2). The conductor-like polarizable continuum model (CPCM) was also used to include the solvent effects of THF.[37] Based on the TD-DFT results, the low-energy absorptions of **2** and **3** are mainly associated with the HOMO−1 → LUMO transition (f > 0.1). While the HOMO−1 for **2** and **3** is predominantly localized on the 2-Ar group of the *o*-carborane (91%, Tables S5 and S9†), the LUMO is delocalized over the central phenylene ring (52% for **2** and 57% for **3**) and carborane cage (38% for **2** and 34% for **3**). This result indicates that the HOMO−1 → LUMO transition in both **2** and **3** is mainly assignable to the π(2-Ar) → π*(phenylene and carborane) ICT transition. This feature could also be characterized by through-space CT transition.[30] In addition, the computed low-energy absorption wavelength for **3** (λ_{abs} = 279 nm) is red-shifted as compared to that for **2** (λ_{abs} = 267 nm), as similarly found in the experimental absorption.

According to the TD-DFT calculations on the S_1 optimized structures of **2** and **3**, the high-energy emission was observed at around 400 nm in both **2** and **3**. The major contribution (f > 0.3) to the emission of **2** and **3** involves HOMO−4 → LUMO and HOMO−6 → LUMO transition, respectively. While both the HOMO−4 (for **2**) and HOMO−6 (for **3**) are mainly located on the central phenylene ring (72–75%) with an appreciable contribution from the carborane cage (23–25%), the LUMOs (for **2** and **3**) are predominantly localized on the carborane cage for both compounds (*ca.* 85%, Table S7 and S11†). As a result, the high-energy emissions can be assigned to partial CT transition from the central phenylene to carborane. 2-Ar groups on the *o*-carboranes have negligible contributions to both transitions, and thus, the transition can be described as local transition centred on the phenylene-carborane fragments. On the other hand, the experimentally observed low-energy AIE in the rigid state of **2** and **3** could be mainly assigned to the HOMO−1 → LUMO transition (λ_{calc} = 484.61 nm for **2** and λ_{calc} = 493.03 nm for **3**). Since the HOMO−1 for **2** and **3** is localized on the 2-Ar groups (91%), this transition involves the π(2-Ar) → π*(phenylene and carborane) ICT transition. Owing to the restricted rotation of the carborane cage, the ICT state may undergo radiative decay in the rigid state.[10,13a,16,18]

Table 2 The major low-energy electronic transition for **2** and **3** at their first excited singlet state (S_1) calculated using the TD-B3LYP method with 6-31G(d) basis sets.[a]

	λ_{calc}/ nm	f	Assignment
2	484.61	0.0006	HOMO−1 → LUMO (99.7%)
	399.88	0.3882	HOMO−4 → LUMO (72.4%) HOMO−5 → LUMO (23.6%)
3	493.03	0.0030	HOMO−1→ LUMO (99.7%)
	386.57	0.4121	HOMO−6 → LUMO (97.3%)

[a] Singlet energies for the vertical transition calculated at the optimized S_1 geometries.

Electron accepting properties of 3. To examine the electron-accepting properties of **3**, the PL spectra of poly(3-hexylthiophene-2,5-diyl) (P3HT) polymer film doped with **3** were investigated (Figure 7). P3HT is well known as a donor for typical electron-accepting materials such as fullerene (C_{60}) derivatives in OPVs. Moreover, the LUMO level (−3.53 eV) of **3**, calculated from CV measurements, is similar to those of fullerene-based acceptors (*ca.* −3.7 eV).[38] The P3HT film itself displayed intense fluorescence in the region between 600 and 800 nm (black line) with excitation at 525 nm, while **3** showed virtually no emission (pink line) at the same excitation (Figure 7). However, as the doping ratios of **3** to P3HT increased, the overall intensity of P3HT emission was gradually quenched. In particular, the PL intensity of the P3HT/**3** film sample with a

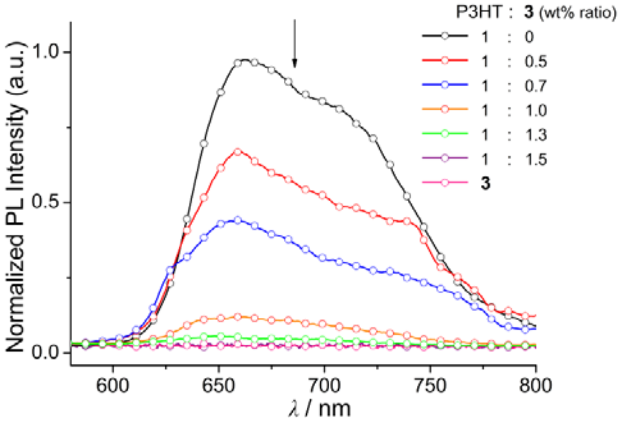

Figure 7. Photoluminescence spectra of P3HT films doped with **3** at 298 K (λ_{ex} = 525 nm).

1:1.5 weight ratio decreased over 97%. In contrast, the absorption bands of the corresponding film samples remained unchanged with the increase in the doping amount of **3** (Figure S8 in the Supporting Information). These results strongly support the fact that photoinduced CT from P3HT (as donor) to **3** (as acceptor) occurs in the P3HT/**3** films, which quenches the P3HT-based fluorescence. This in turn indicates that the excited electrons in the LUMO of P3HT (*ca*. −3.3 to −3.5 eV) can easily move to the LUMOs of **3**. Accordingly, it is expected that the tris-carborane compound **3** could be utilized as a potential electron-accepting or absorbing material in optoelectronic applications.

Conclusions

We have prepared and characterized mono-, bis- and tris-*o*-carborane-substituted benzene compounds (**1**–**3**). While the mono-substituted compound **1** was non-emissive in solution state at 298 K, **2** and **3** showed weak to moderate emission in the high-energy region. Compounds **2** and **3** exhibited dual emission bands at 77 K and in film, of which the broad low-energy emission band was dominantly observed in the solid state. Computational studies suggested that the additional low-energy emission in **2** and **3** was involved with the ICT state. The emission was also assigned to AIE in nature, showing enhanced emission intensity upon increasing water fraction in THF/water mixtures. Finally, PL experiments using P3HT polymer film doped with **3** showed the excellent electron-accepting properties of **3**.

Experimental Section

General considerations. All operations were performed under an inert nitrogen atmosphere using standard Schlenk and glove box techniques. Anhydrous grade solvents (Sigma Aldrich) were dried by passing through an activated alumina column and stored over activated molecular sieves (5 Å). Spectrophotometric-grade tetrahydrofuran (THF) was used as received from Sigma Aldrich. The following commercial reagents were used without any further purification after purchasing from Sigma Aldrich: bis(triphenylphosphine)palladium(II) dichloride, copper(I) iodide, *n*-butyllithium hexane solution (2.5M), diethyl sulfide, triethylamine, 4-butylphenylacetylene, bromobenzene, 1,3-dibromobenzene, 1,3,5-tribromobenzene, poly(3-hexylthiophene-2,5-diyl). Decaborane ($B_{10}H_{14}$) was purchased from KatChem and used without further purification. $CDCl_3$ (Cambridge Isotope Laboratories) was used after drying over activated molecular sieves (5 Å). NMR spectra were recorded on a Bruker Avance 400 spectrometer (400.13 MHz for ^{1}H, 100.62 MHz for ^{13}C, and 128.38 MHz for ^{11}B) at ambient temperature unless otherwise stated. Chemical shifts are given in ppm, and are referenced against external Me_4Si (^{1}H, ^{13}C) and $BF_3{\cdot}Et_2O$ (^{11}B). HRMS (EI) measurement (JEOL JMS700) was carried out at Korea Basic Science Institute. Elemental analyses were performed on an EA3000 (Eurovector) in the Central Laboratory of Kangwon National University. UV/Vis absorption and PL spectra were recorded on a Jasco V-530 and a Spex Fluorog-3 luminescence spectrophotometer, respectively. Thermogravimetric analysis (TGA) was obtained using a TA Q500 under a flow of dry nitrogen with a heating rate of 10 °C/min. T_{d5} values of **2** and **3** were determined by TGA at 5% weight loss. Cyclic voltammetry (CV) experiments were performed using a Metrohm Autolab PGSTAT12 system.

Synthesis of 1-butyl-4-(phenylethynyl)benzene (1a). To the mixture of bromobenzene (0.50 g, 3.18 mmol), copper iodide (80 mg), and $Pd(PPh_3)_2Cl_2$ (120 mg) in 10 mL of toluene was added triethylamine (90 mL) at room temperature. After stirring for 15 min, 4-butylphenylacetylene (0.68 mL, 3.81 mmol) in toluene (10 mL) was added to the resulting dark brown slurry. The reaction mixture was then refluxed for 24 h. All the volatiles were removed at reduced pressure, affording gray oily residue. Purification was carried out by column chromatography (silica gel, CH_2Cl_2/hexane as an eluent) to afford the desired product **1a** as a pale yellow oil (0.32 g, 43%). ^{1}H NMR ($CDCl_3$): δ 7.50 (d, J = 8.0 Hz, 2H, C_6H_4), 7.42 (d, J = 8.0 Hz, 2H, C_6H_4), 7.31 (d, J = 7.6 Hz, 2H, Ph-*H*), 7.30 (t, J = 8.2 Hz, 1H, Ph-*H*), 7.14 (d, J = 8.0 Hz, 2H, Ph-*H*), 2.60 (t, J = 15.6 Hz, 2H of *n*-butyl), 1.58 (m, 2H of *n*-butyl), 1.33 (m, 2H of *n*-butyl), 0.91 (t, J = 14.8 Hz, 3H of *n*-butyl). ^{13}C NMR ($CDCl_3$): δ 143.41, 131.56, 131.52, 128.48, 128.32, 128.06, 123.53, 120.40, 89.62 (Acetylene-*C*), 88.73 (Acetylene-*C*), 35.62, 33.42, 22.33, 13.96.

Synthesis of 1,3-Bis(2-(4-Butylphenylacetylenyl)benzene (2a). This compound was prepared in a manner analogous to the synthesis of **1a** using 1,3-dibromobenzene. Purification was carried out by column chromatography (silica gel, CH_2Cl_2/hexane as an eluent) to afford the desired product as a pale gray solid (0.43 g, 55%). ^{1}H NMR ($CDCl_3$): δ 7.68 (s, 1H, C_6H_4), 7.45 (dd, J = 9.2 Hz, 2H, C_6H_4), 7.42 (d, J = 8.0 Hz, 4H, Ph-*H*), 7.30 (t, J = 7.6 Hz, 1H, C_6H_4), 7.15 (d, J = 8.0 Hz, 4H, Ph-*H*), 2.61 (t, J = 12.0 Hz, 4H of *n*-butyl), 1.59 (m, 4H of *n*-butyl), 1.33 (m, 4H of *n*-butyl), 0.92 (t, J = 14.8 Hz, 6H of *n*-butyl). ^{13}C NMR ($CDCl_3$): δ 143.57, 134.47, 131.53, 131.01, 128.48, 128.36, 123.79, 120.13, 90.13 (Acetylene-*C*), 87.95 (Acetylene-*C*), 35.60, 33.38, 22.30, 13.92. Anal. Calcd for $C_{30}H_{30}$: C, 92.26; H, 7.74. Found: C, 91.93; H, 7.50.

Synthesis of 1,3,5-Tris(2-(4-butylphenylacetylenyl)benzene (3a). This compound was prepared in a manner analogous to the synthesis of **1a** using 1,3,5-tribromobenzene. Purification was carried out by column chromatography (silica gel, hexane) to afford the desired product as a colorless oil (0.48 g, 62%). ^{1}H NMR ($CDCl_3$): δ 7.62 (s, 3H, C_6H_3), 7.45 (d, J = 8.0 Hz, 6H, Ph-*H*), 7.17 (d, J = 7.6 Hz, 6H, Ph-*H*), 2.63 (t, J = 15.6 Hz, 6H of *n*-butyl), 1.61 (m, 6H of *n*-butyl), 1.36 (m, 6H of *n*-butyl), 0.94 (t, J = 14.4 Hz, 9H of *n*-butyl). ^{13}C NMR ($CDCl_3$): δ 143.71, 133.72, 131.57, 128.49, 124.13, 119.93, 90.62 (Acetylene-*C*), 87.30 (Acetylene-*C*), 35.60, 33.35, 22.29, 13.91; Anal. Calcd for $C_{42}H_{38}$: C, 92.94; H, 7.06. Found: C, 92.51; H, 7.11.

Synthesis of 2-(4-Butylphenyl)-*o*-carboran-1-yl)benzene (1). To a toluene solution (100 mL) of decaborane ($B_{10}H_{14}$, 0.13 g, 1.06 mmol) and **1a** (0.21 g, 0.89 mmol) was added an excess amount of Et_2S (5 equiv) at room temperature. After heating to reflux, the reaction mixture was further stirred for 3 days. The solvent was removed under vacuum. The solution was purified by column chromatography on alumina using toluene/*n*-hexane as an eluent, affording **1** as a pale yellow oil (0.17 g, 54%). ^{1}H NMR ($CDCl_3$): δ 7.39 (d, J = 8.4 Hz, 2H), 7.28 (d, J = 8.4 Hz, 2H), 7.21 (t, J = 14.8, 1H), 7.11 (t, J = 15.2 Hz, 2H), 6.90 (d, J = 8.4 Hz, 2H), 3.30-1.50 (br, 10H, CB-*H*), 2.45 (t, J = 15.6 Hz, 2H of *n*-butyl), 1.45 (m, 2H of *n*-butyl), 1.20 (m, 2H of *n*-butyl), 0.83 (t, J = 14.4 Hz, 3H of *n*-butyl). ^{13}C NMR ($CDCl_3$): δ 145.29, 130.76, 130.62, 130.49, 130.01, 128.24, 128.17, 127.96, 85.56 (CB-*C*), 85.20 (CB-*C*), 34.96, 32.97, 22.14, 13.87. ^{11}B NMR (acetone-d_6, 25 °C): δ –2.4 (br d, $^1J_{B\text{-}H}$ = 153.5 Hz, 3B), –9.9 (overlapping dd, $^1J_{B\text{-}H}$ = 166.4 Hz, 7B). HRMS (EI): *m/z* Calcd for $C_{18}H_{28}B_{10}$: 354.3122. Found: 354.3123.

Synthesis of 1,3-Bis(2-(4-butylphenyl)-*o*-carboran-1-yl)benzene (2). This compound was prepared in a manner analogous to the synthesis of

1 using **2a**. After heating to reflux, the reaction mixture was further stirred for 3 days. The solvent was removed under vacuum and MeOH (50 mL) was added to the residue. The resulting yellow slurry was filtered and the remaining solid was re-dissolved in toluene. The solution was purified by column chromatography on alumina using toluene as an eluent. Recrystallization from a mixture of CH_2Cl_2/*n*-hexane afforded **2** as a white solid (0.48 g, 33%). Single crystals suitable for X-ray diffraction studies were grown from cooling of a CH_2Cl_2/*n*-hexane solution of **2**. ^{1}H NMR ($CDCl_3$): δ 7.28 (s, 1H, C_6H_4), 7.25 (dd, *J* = 6.4 Hz, 2H, C_6H_4), 7.17 (d, *J* = 8.4 Hz, 4H, CB-Ph-*H*), 6.93 (d, *J* = 8.4 Hz, 4H, CB-Ph-*H*), 6.92 (t, *J* = 11.2 Hz, 1H, C_6H_4), 3.30-1.50 (br, 20H, CB-*H*), 2.48 (t, *J* = 15.6 Hz, 4H of *n*-butyl), 1.48 (m, 4H of *n*-butyl), 1.24 (m, 4H of *n*-butyl), 0.86 (t, *J* = 14.8 Hz, 6H of *n*-butyl). ^{13}C NMR ($CDCl_3$): *δ* 145.73, 132.21, 131.94, 130.82, 130.37, 128.49, 128.18, 127.49, 85.27 (CB-*C*), 83.20 (CB-*C*), 35.00, 32.97, 22.25, 13.83. ^{11}B NMR (acetone-d_6, 60 °C): *δ* –1.8 – –3.5 (br m, 6B), –9.9 (overlapping dd, $^1J_{B\text{-}H}$ = 147.7 Hz, 14B). Anal. Calcd for $C_{30}H_{50}B_{20}$: C, 57.47; H, 8.04. Found: C, 57.10; H, 7.89. HRMS (EI): *m/z* Calcd for $C_{30}H_{50}B_{20}$: 630.5774. Found: 630.5778.

Synthesis of 1,3,5-Tris(2-(4-butylphenyl)-*o*-carboran-1-yl)benzene (3). This compound was prepared in a manner analogous to the synthesis of **2** using **3a**. Recrystallization from a solution of CH_2Cl_2/*n*-hexane afforded **3** as a white solid (0.23 g, 46%). ^{1}H NMR ($CDCl_3$): *δ* 7.15 (s, 3H, C_6H_3), 7.03 (d, *J* = 8.4 Hz, 6H, CB-Ph-*H*), 6.94 (d, *J* = 8.4 Hz, 6H, CB-Ph-*H*), 3.30-1.50 (br, 30H, CB-*H*), 2.50 (t, *J* = 16.0 Hz, 6H of *n*-butyl), 1.50 (m, 6H of *n*-butyl), 1.28 (m, 6H of *n*-butyl), 0.88 (t, *J* = 14.8 Hz, 9H of *n*-butyl). ^{13}C NMR ($CDCl_3$): *δ* 146.10, 133.37, 131.11, 130.26, 128.66, 127.15, 84.93 (CB-*C*), 81.51 (CB-*C*), 35.10, 33.01, 22.45, 13.84. ^{11}B NMR (acetone-d_6, 60 °C): *δ* –2.6 (overlapping dd, $^1J_{B\text{-}H}$ = 126.1 Hz, 9B), –10.3 (br d, $^1J_{B\text{-}H}$ = 146.7 Hz, 21B). Anal. Calcd for $C_{42}H_{72}B_{30}$: C, 55.97; H, 8.05. Found: C, 55.85; H, 8.17. HRMS (EI): *m/z* Calcd for $C_{42}H_{72}B_{30}$: 906.8426. Found: 906.8431.

X-ray crystallography. Single crystals of **2** and **3** were coated with Paratone oil and mounted onto a glass capillary. The crystallographic measurements were carried out using a Bruker SMART Apex II CCD area detector diffractometer with a graphite-monochromated Mo-Kα radiation (λ = 0.71073 Å). The structures were solved by direct methods and all non-hydrogen atoms were subjected to anisotropic refinement by a full-matrix least-squares method on F^2 by using the SHELXTL/PC package, resulting in X-ray crystallographic data of **2** and **3** in CIF format (CCDC 1463120 and 1032713). Hydrogen atoms were placed at their geometrically calculated positions and refined riding on the corresponding carbon atoms with isotropic thermal parameters. The detailed crystallographic data, bond lengths and angles are given in Table S1 and S2†.

Theoretical calculations. The geometries of **2** and **3** were optimized using the density functional theory (DFT) method with the B3LYP functional[39] and 6-31G(d)[40] basis sets. The electronic transition energies including an account of electron correlation for **2** and **3** were obtained by time-dependent density functional theory (TD-DFT)[41] measurements using the hybrid B3LYP functional (TD-B3LYP). The conductor-like polarizable continuum model (CPCM) was used to include the solvent effects of THF.[37] The calculations were carried out using the GAUSSIAN 09 program.[42] The GaussSum 3.0 was used to calculate the percent contribution of a fragment to each molecular orbital in the molecule.[43]

Cyclic voltammetry. Cyclic voltammetry measurements of **1**–**3** were performed by a three-electrode cell configuration system consisting of platinum working and counter electrodes and a Ag/$AgNO_3$ (0.1 M in CH_3CN) reference electrode at room temperature. The solvent was dimethyl sulfoxide (DMSO) and 0.1 M tetrabutylammonium hexafluorophosphate was used as the supporting electrolyte. All solvents were sufficiently degassed during 1 h before use. The reduction potentials were recorded at a scan rate of 100 mV/s and reported with reference to the ferrocene/ferrocenium (Fc/Fc^+) redox couple.

UV/Vis absorption and photoluminescence (PL) experiments. UV/Vis absorption and PL measurements in solution (5×10^{-5} M) were performed with a 1-cm quartz cuvette. The solution quantum efficiencies were measured with reference to that of quinine sulfate (0.5 M H_2SO_4, Φ = 0.55).[44] The absolute photoluminescence quantum yields (PLQYs) of **2** and **3** in the solid state were obtained using an absolute PL quantum yield spectrophotometer (Quantaurus-QY C11347-11, Hamamatsu Photonics) equipped with a 3.3 inch integrating sphere at 298 K. The thin film samples in PMMA were obtained from spin-coating of a THF solution (1 mL) of PMMA (50 mg) containing *o*-carborane compounds (20 wt% versus PMMA) on 15 × 15 mm quartz plate (thickness = 1 mm). P3HT films doped with **3** were obtained from spin-coating of $CHCl_3$ solutions (1 mL) containing P3HT (10 mg) and 0 – 1.5 wt% of **3**.

Acknowledgements

This research was supported by the Nano·Material Technology Development Program (NRF-2016M3A7B4909246 for K. M. Lee) and Basic Science Research Program (NRF-2016R1C1B1008452 for M. H. Park) through the National Research Foundation of Korea (NRF) funded by the Ministry of Science, ICT & Future Planning. M. H. Lee is thankful for the Priority Research Centers program (2009-0093818) through the NRF funded by the Ministry of Education. K. M. Lee thanks the support from the 2015 Research Grant from Kangwon National University.

Keywords: Carboranes • Charge transfer • Cyclic voltammetry • Luminescence • Photophysics

[1] a) R. N. Grimes, *Carboranes*, 2nd ed. Academic Press, London, **2011**; b) A. M. Spokoyny, *Pure Appl. Chem.* **2013**, *85*, 903–919.

[2] a) R. M. Dziedzic, L. M. A. Saleh, J. C. Axtell, J. L. Martin, S. L. Stevens, A. T. Royappa, A. L. Rheingold, A. M. Spokoyny, *J. Am. Chem. Soc.* **2016**, *138*, 9081−9084; b) K. O. Kirlikovali, J. C. Axtell, A. Gonzalez, A. C. Phung, S. I. Khan, A. M. Spokoyny, *Chem. Sci.* **2016**, *7*, 5132–5138; c) L. M. A. Saleh, R. M. Dziedzic, S. I. Khan, A. M. Spokoyny, *Chem. Eur. J.* **2016**, *22*, 8466‑8470; d) B. J. Eleazer, M. D. Smith, A. A. Popov, D. V. Peryshkov, *J. Am. Chem. Soc.* **2016**, *138*, 10531–10538; e) Y. O. Wong, M. D. Smith, D. V. Peryshkov, *Chem. Eur. J.* **2016**, *22*, 6764–6767; f) A. L. Chan, J. Estrada, C. E. Kefalidis, V. Lavallo, *Organometallics* **2016**, *35*, 3257–3260; g) S. P. Fisher, A. El-Hellani, F. S. Thama, V. Lavallo, *Dalton Trans.* **2016**, *45*, 9762–9765; h) R. Núñez, I. Romero, F. Teixidor and C. Viñas, *Chem. Soc. Rev.* **2016**, *45*, 5147–5173; i) M. J. Asay, S. P. Fisher, S. E. Lee, F. S. Tham, D. Borchardt, V. Lavallo, *Chem. Commun.* **2015**, *51*, 5359–5362.

[3] a) R. Núñez, M. Tarrés, A. Ferrer-Ugalde, F. F. D. Biani and F. Teixidor, *Chem. Rev.* **2016**, *116*, 14307–14378; b) S. Mukherjee, P. Thilagar, *Chem. Commun.* **2016**, *52*, 1070–1093 and references therein.

[4] a) Y. Kim, S. Park, Y. H. Lee, J. Jung, S. Yoo, M. H. Lee, *Inorg. Chem.* **2016**, *55*, 909–917; b) Y. H. Lee, J. Park, S.-J. Jo, M. Kim, J. Lee, S. U. Lee, M. H. Lee, *Chem. Eur. J.* **2015**, *21*, 2052–2061; *c*). K.-R. Wee, Y.-J. Cho, S. Jeong, S. Kwon, J.-D. Lee, I.-H. Suh, S. O. Kang, *J. Am. Chem. Soc.* **2012**, *134*, 17892–17990.

[5] a) H. J. Bae, J. Chung, H. Kim, J. Park, K. M. Lee, T.-W. Koh, Y. S. Lee, S. Yoo, Y. Do, M. H. Lee, *Inorg. Chem.* **2014**, *53*, 128–138; b) T. Kim, H. Kim, K. M. Lee, Y. S. Lee, M. H. Lee, *Inorg. Chem.* **2013**, *52*, 160–168.

[6] a) R. N. Grimes, *Dalton Trans.* **2015**, *44*, 5939–5956; b) Z.-J. Yao, G.-X. Jin, *Coord. Chem. Rev.* **2013**, *257*, 2522–2535; c) A. M. Spokoyny, *Pure Appl. Chem.* **2013**, *85*, 903–919; d) N. S. Hosmane, *Boron Science: New Technologies and Applications*, CRC Press, New York, **2012**; e) R. N. Grimes, *Carboranes*, Academic Press, London, **2011**; f) A. S. Weller, *Nat. Chem.* **2011**, *3*, 577–578; g) R. Núñez, P. Farràs, F. Teixidor, C. Viñas, R. Sillanpää and R. Kivekäs, *Angew. Chem. Int. Ed.* **2006**, *45*, 1270–1272; h) Z. Chen, R. B. King, *Chem. Rev.* **2005**, *105*, 3613–3642; i) R. B. King, *Chem. Rev.* **2001**, *101*, 1119–1152; j) V. I. Bregadze, *Chem. Rev.* **1992**, *92*, 209–223; k) R. E. Williams, *Chem. Rev.* **1992**, *92*, 177–207.

[7] a) H. Naito, Y. Morisaki, Y. Chujo, *Angew. Chem. Int. Ed.* **2015**, *54*, 5084–5087; b) T. Kim, J. Lee, S. U. Lee, M. H. Lee, *Organometallics* **2015**, *34*, 3455–3458; c) H. J. Bae, H. Kim, K. M. Lee, T. Kim, M. Eo, Y. S. Lee, Y. Do, M. H. Lee, *Dalton Trans.* **2013**, *42*, 8549–8552.

[8] J. Park, Y. H. Lee, J. Y. Ryu, J. Lee, M. H. Lee, *Dalton Trans.* **2016**, *45*, 5667–5675.

[9] X. Li, H. Yan, Q. Zhao, *Chem. Eur. J.* **2016**, *22*, 1888–1898 and references therein.

[10] Y. H. Lee, J. Park, J. Lee, S. U. Lee, M. H. Lee, *J. Am. Chem. Soc.* **2015**, *137*, 8018–8021.

[11] A. M. Prokhorov, T. Hofbeck, R. Czerwieniec, A. F. Suleymanova, D. N. Kozhevnikov, H. Yersin, *J. Am. Chem. Soc.* **2014**, *136*, 9637–9642.

[12] a) C. Shi, H. Sun, X. Tang, W. Lv, H. Yan, Q. Zhao, J. Wang, W. Huang, *Angew. Chem., Int. Ed.* **2013**, *52*, 13434–13438; b) C. Shi, H. Sun, Q. Jiang, Q. Zhao, J. Wang, W. Huang, H. Yan, *Chem. Commun.* **2013**, *49*, 4746–4748.

[13] a) B. H. Choi, J. H. Lee, H. Hwang, K. M. Lee, M. H. Park, *Organometallics* **2016**, *35*, 1771–1777; b) J. Cabrera-González, C. Viñas, M. Haukka, S. Bhattacharyya, J. Gierschner and R. Núñez, *Chem. Eur. J.* **2016**, *22*, 1–12; c) A. González-Campo, A. Ferrer-Ugalde, C. Viñas, F. Teixidor, R. Sillanpää, J. Rodríguez-Romero, R. Santillan, N. Farfán and R. Núñez, *Chem. Eur. J.* **2013**, *19*, 6299–6312.

[14] S. Kwon, K.-R. Wee, Y.-J. Cho, S. O. Kang, *Chem. Eur. J.* **2014**, *20*, 5953–5960.

[15] K.-R. Wee, W.-S. Han, D. W. Cho, S. Kwon, C. Pac, S. O. Kang, *Angew. Chem., Int. Ed.* **2012**, *51*, 2677–2680.

[16] L. Weber, J. Kahlert, R. Brockhinke, L. Böhling, A. Brockhinke, H.-G. Stammler, B. Neumann, R. A. Harder, M. A. Fox, *Chem. Eur. J.* **2012**, *18*, 8347–8357.

[17] a) L. Weber, J. Kahlert, R. Brockhinke, L. Böhling, J. Halama, A. Brockhinke, H.-G. Stammler, B. Neumann, C. Nervi, R. A. Harder. M. A. Fox, *Dalton Trans.* **2013**, *42*, 10982–10996; b) L. Weber, J. Kahlert, L. Böhling, A. Brockhinke, H.-G. Stammler, B. Neumann, R. A. Harder, P. J. Low, M. A. Fox, *Dalton Trans.* **2013**, *42*, 2266–2281.

[18] H. J. Bae, H. Kim, K. M. Lee, T. Kim, Y. S. Lee, Y. Do, M. H. Lee, *Dalton Trans.* **2014**, *43*, 4978–4985.

[19] J. Kahlert, L. Böhling, A. Brockhinke, H.-G. Stammler, B. Neumann, L. M. Rendina, P. J. Low, L. Weber, M. A. Fox, *Dalton Trans.* **2015**, *44*, 9766–9781.

[20] S.-Y. Kim, Y.-J. Cho, G. F. Jin, W.-S. Han, H.-J, Son, D. W. Cho, S. O. Kang, *Phys. Chem. Chem. Phys.* **2015**, *17*, 15679–15682.

[21] S.-Y. Kim. A.-R. Lee, Y.-J. Cho, H.-J. Son, W.-S. Han, S. O. Kang, *J. Organomet. Chem.* **2015**, *798*, 245–251.

[22] K.-R. Wee, Y.-J. Cho, J. K. Son, S. O. Kang, *Angew. Chem. Int. Ed.* **2013**, *52*, 9682–9685.

[23] M. Tominaga, H. Naito, Y. Morisaki, Y. Chujo, *Asian J. Org. Chem.* **2014**, *3*, 624–631.

[24] M. Tominaga, H. Naito, Y. Morisaki, Y. Chujo, *New J. Chem.* **2014**, *38*, 5686–5690.

[25] L. Böhling, A. Brockhinke, J. Kahlert, L. Weber, R. A. Harder, D. S. Yufit, J. A. K. MacBride, M. A. Fox, *Eur. J. Inorg. Chem.* **2016**, 430–412.

[26] a) J. Guo, D. Liu, J. Zhang, J. Zhang, Q. Miao, Z. Xie, *Chem. Commun.* **2015**, *51*, 12004–12007; b) S.-Y. Kim, A.-R. Lee, G. F. Jin, Y.-J. Cho, H.-J. Son, W.-S. Han, S. O. Kang, *J. Org. Chem.* **2015**, *80*, 4573–4580; c) G. F. Jin, J.-H. Hwang, J. D. Lee, K.-R. Wee, I.-H. Suh, S. O. Kang, *Chem. Commun.* **2013**, *49*, 9398–9400; d) M. Eo, H. J. Bae, M. Hong, Y. Do, S. Cho, M. H. Lee, *Dalton Trans.* **2013**, *42*, 8104–8112.

[27] A. R. Garber, G. M. Bodner, L. J. Todd, *J. Magn. Reson.* **1977**, *28*, 383–390.

[28] C. Songkram, K. Takaishi, K. Yamaguchi, H. Kagechika, Y. Endo, *Tetrahedron Lett.* **2001**, *42*, 6365–6368.

[29] a) K. M. Lee, J. O. Huh, T. Kim, Y. Do, M. H. Lee, *Dalton Trans.* **2011**, *40*, 11758–11764; b) H. Tricas, M. Colon, D. Ellis, S. A. Macgregor, D. McKay, G. M. Rosair, A. J. Welch, I. V. Glukhov, F. Rossi, F. Laschi, P. Zanello, *Dalton Trans.* **2011**, *40*, 4200–4211.

[30] J. O. Huh, H. Kim, K. M. Lee, Y. S. Lee, Y. Do, M. H. Lee, *Chem. Commun.* **2010**, *46*, 1138–1140.

[31] K. C. Song, H. Kim, K. M. Lee, Y. S. Lee, Y. Do, M. H. Lee, *Dalton Trans.* **2013**, *42*, 2351–2354.

[32] a) A. Ferrer-Ugalde, A. González-Campo, C. Viñas, J. Rodríguez-Romero, R. Santillan, N. Farfán, R. Sillanpää, A. Sousa-Pedrares, R. Núñez, and F. Teixidor, *Chem. Eur. J.*, 2014, **20**, 9940–9951; b) A. Ferrer-Ugalde, E. J. Juárez-Pérez, F. Teixidor, C. Viñas, R. Sillanpää, E. Pérez-Inestrosa, R. Núñez, *Chem. Eur. J.* **2012**, *18*, 544–553.

[33] K. Kokado, Y. Chujo, *J. Org. Chem.*, **2011**, *76*, 316–319.

[34] a) B. P. Dash, R. Satapathy, E. R. Gaillard, K. M. Norton, J. A. Maguire, N. Chug, N. S. Hosmane, *Inorg. Chem.* **2011**, *50*, 5485–5493; b) B. P. Dash, R. Satapathy, E. R. Gaillard, J. A. Maguire, N. S. Hosmane, *J. Am. Chem. Soc.* **2010**, *132*, 6578–6587.

[35] F. Lerouge, A. Ferrer-Ugalde, C. Viñas, F. Teixidor, R. Sillanpää, A. Abreu, E. Xochitiotzi, N. Farfán, R. Santillan, R. Núñez, *Dalton Trans.* **2011**, *40*, 7541–7550.

[36] Y. C. Simon, J. J. Peterson, C. Mangold, K. R. Carter, E. B. Coughlin, *Macromolecules* **2008**, *42*, 512–516.

[37] a) M. Cossi, N. Rega, G. Scalmani, V. Barone, *J. Comput. Chem.* **2003**, *24*, 669–681; b) V. Barone, M. Cossi, *J. Phys. Chem. A* **1998**, *102*, 1995–2001.

[38] F. Matsumoto, T. Iwai, K. Moriwaki, Y. Takao, T. Ito, T. Mizuno, T. Ohno, *J. Org. Chem.* **2012**, *77*, 9038–9043.

[39] a) P. J. Stephens, F. J. Devlin, C. F. Chabalowski, M. J. Frisch, *J. Phys. Chem.* **1994**, *98*, 11623–11627; b) C. Lee, W. Yang, R. G. Parr, *Phys. Rev. B: Condens. Matter* **1988**, *37*, 785–789.

[40] J. S. Binkley, J. A. Pople, W. J. Hehre, *J. Am. Chem. Soc.* **1980**, *102*, 939–947.

[41] E. Runge, E. K. U. Gross, *Phys. Rev. Lett.* **1984**, *52*, 997–1000.

[42] M. J. Frisch, G. W. Trucks, H. B. Schlegel, G. E. Scuseria, M. A. Robb, J. R. Cheeseman, G. Scalmani, V. Barone, B. Mennucci, G. A. Petersson, H. Nakatsuji, M. Caricato, X. Li, H. P. Hratchian, A. F. Izmaylov, J. Bloino, G. Zheng, J. L. Sonnenberg, M. Hada, M. Ehara, K. Toyota, R. Fukuda, J. Hasegawa, M. Ishida, T. Nakajima, Y. Honda, O. Kitao, H. Nakai, T. Vreven, J. A. Montgomery, Jr., J. E. Peralta, F. Ogliaro, M. Bearpark, J. J. Heyd, E. Brothers, K. N. Kudin, V. N. Staroverov, T. Keith, R. Kobayashi, J. Normand, K. Raghavachari, A. Rendell, J. C. Burant, S. S. Iyengar, J. Tomasi, M. Cossi, N. Rega, J. M. Millam, M. Klene, J. E. Knox, J. B. Cross, V. Bakken, C. Adamo, J. Jaramillo, R. Gomperts, R. E. Stratmann, O. Yazyev, A. J. Austin, R. Cammi, C. Pomelli, J. W. Ochterski, R. L. Martin, K. Morokuma, V. G. Zakrzewski, G. A. Voth, P. Salvador, J. J. Dannenberg, S. Dapprich, A. D. Daniels, O. Farkas, J. B. Foresman, J. V. Ortiz, J. Cioslowski, D. J. Fox, *Gaussian 09 Revision D.01; Gaussian. Inc.: Wallingford*, CT, **2013**.

[43] N. M. O'Boyle, A. L. Tenderholt, K. M. Langner. *J. Comp. Chem.* **2008**, *29*, 839–845.

[44] a) A. M. Brouwer, *Pure Appl. Chem.* **2011**, *83*, 2213–2228; b) W. H. Melhuish, *J. Phys. Chem.* **1961**, *65*, 229–235.

FULL PAPER

Multiple *o*-carborane substituted compounds, mono-, 1,3-bis-, and 1,3,5-tris-(2-(4-butylphenyl)-*o*-carboran-1-yl)benzene (**1**–**3**), were prepared and characterized. Various photophysical properties of these series were investigated.

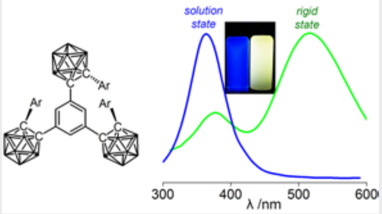

multi-carborane

Dong Kyun You, Ji Hye Lee, Byung Hoon Choi, Hyonseok Hwang, Min Hyung Lee, Kang Mun Lee* and Myung Hwan Park**

Page No. – Page No.

Effects of multi-carborane substitution on the photophysical and electron accepting properties of *o*-carboranylbenzene compounds